

CAVITATION AND EROSION RESISTANCE OF VACUUM ARC Ti, Ti-Al, Ti-Zr, AND Ti-Ni COATINGS

I.O. Klimenko, V.G. Marinin, M.A. Bortnitskaya, A.S. Kuprin

National Science Center “Kharkov Institute of Physics and Technology”, Kharkiv, Ukraine

E-mail: klimenko@kipt.kharkov.ua

Studies on the influence of technological parameters (cathode-substrate distance, substrate temperature, bias voltage, arc current) of vacuum-arc titanium deposition coatings have shown that the deposition rate from one cathode is inversely proportional to the square of the distance between the sample and the cathode surface and proportional to the angle of inclination of the sample relative to the normal to the cathode surface. Sputtered titanium coatings at optimal parameters have 1.25 times higher cavitation resistance than bulk titanium. Among the alloyed vacuum-arc coatings TiAl, TiZr, and TiNi, coatings of the TiAl and TiNi systems have the highest resistance to cavitation and abrasive wear.

INTRODUCTION

Cavitation erosion is an example of a serious material wear problem in systems subjected to hydrodynamic turbulence: hydraulic machine components, propellers and turbine parts. The mechanism of cavitation erosion involves the action of bubbles in the resulting liquids, and then break down on the surface of the material as a result of rapid pressure changes [1, 2].

Titanium and its alloys have a fairly high resistance to cavitation damage [3–6], and for further improvement, surface modification methods are used: ion-plasma treatment and protective coatings [7].

Results of cavitation stability PVD coatings for the various materials protection studies are given in reviews [8, 9]. However, these works provide data mainly on the protective properties of nitride (TiN, CrN, TiAlN), carbide (WC, WC/aC:H), and carbonitride (CrCN) coatings. In the literature, there is almost no data on the cavitation resistance of metal vacuum-arc titanium coatings without the addition of nitrogen, and the available data refer to coatings obtained from a plasma flow with separation of macroparticles [10]. Vacuum-arc plasma sources with separation from macroparticles cannot be or economically unreasonable to use for the deposition of protective coatings on large-sized products (for example, the blades of the last stages of steam turbines) [11].

Massive samples of alloys [12] and plasma coatings [13] of the Ti-Ni system have high cavitation and corrosion resistance, resistance to stress corrosion cracking, strength and ductility. It was found in [14] that NiTi thin coatings deposited from filtered vacuum arc plasma showed better cavitation erosion resistance compared to 316 austenitic stainless steel. Improved cavitation erosion resistance by pseudoelasticity of NiTi thin film.

The purpose of this work is to investigate the effect of deposition process parameters (cathode-substrate distance, substrate temperature, bias voltage, arc current), as well as the effect of doping with aluminum, zirconium, and nickel on the cavitation resistance of vacuum-arc titanium coatings. The choice of aluminum, zirconium and nickel as alloying elements is due to the fact that they

affect the structure and properties of titanium in different ways.

MATERIALS AND EXPERIMENTAL TECHNIQUE

Coatings were deposited using a vacuum arc discharge on a Bulat-type installation [11]. The cathodes were made of VT1-0 titanium. The arc discharge current was varied in the range from 65 to 135 A, and the negative bias potential was up to 200 V. The initial pressure in the vacuum chamber was $8 \cdot 10^{-4}$ Pa, and after the plasma source was operated for 1 h, it was $2 \cdot 10^{-4}$ Pa. Coatings were deposited on polished plates made of Cr18Ni10Ti steel. The plates were placed at different distances from the cathode, in particular, at a distance L_0 from the cathode along the normal to it, as well as at a fixed value l at different distances from the axis parallel to the cathode surface and at an angle to it.

The Ti-Al coating was deposited using a single Ti-8Al alloy cathode or two Ti and Al cathodes. Coating formation conditions: negative substrate potential 200 and current on the Al cathode 70 A; current at Ti cathode 100...120 A; gas pressure (Ar) in the vacuum chamber $8 \cdot 10^{-3}$, 0.8 Pa, respectively. The deposition of Ti-Zr coatings was carried out with the simultaneous operation of two Ti and Zr plasma sources located at an angle of 90° to each other and at 45° angle to the substrate to be coated. The Ti-Ni coating was deposited in a vacuum of $6 \cdot 10^{-4}$ Pa from two plasma sources located towards each other. The current of each of the cathodes is 100 A, the negative bias potential on the substrates is 100 V. The coating thickness is from 10 to 20 μm . By varying the current I_d at the cathodes in each plasma source, the composition of the coating was controlled. The temperature of the sample during the formation of coatings was measured using a chromel-alumel thermocouple.

The cavitation wear of samples with coatings was measured on a setup described in [3]. During its operation, the signal from the generator of ultrasonic oscillations was applied to a magnetostrictive transducer mechanically connected to an exponential profile concentrator. A zone with developed cavitation was formed under the end surface of the concentrator. The

amplitude of oscillations of the end surface of the concentrator was equal to $(30 \pm 2) \mu\text{m}$, and the frequency was 20 kHz. The erosion of the samples was measured gravimetrically using a VLR-20 balance with an accuracy of $\pm 0.015 \text{ mg}$. Based on the experimental data, kinetic curves were built in the coordinates “weight loss – time of cavitation”. The average destruction rate (V_0) was determined from the slope of the tangent to the kinetic curve on the segment characterizing a linear or close dependence. The cavitation resistance (Z_h) was calculated from the rate of destruction.

The mass loss of the coating due to the action of the abrasive was determined by the interaction of the disk with abrasive particles and the applied coating on the plane. The speed of movement of the surface of the disk in contact with the coating is equal to 4.38 m/s at a load of the coated sample of 2.2 N. The mass loss of the coating was measured over a fixed period of time.

Detailed metallographic studies of the coatings structure were carried out using optical microscopy. X-ray diffraction studies were carried out on a DRON-3 diffractometer. The microhardness of the coatings was measured using a PMT-3 microhardness tester at a load of 1 N.

EXPERIMENTAL RESULTS

The influence of the arc discharge current, the negative potential on the substrate, and the pressure in the vacuum chamber of $2 \cdot 10^{-4} \text{ Pa}$, at which the coating is formed, and the deposition temperature were studied. The results of studies for the option of placing the substrates on which coatings are deposited along the normal to the cathode surface are shown in Fig. 1. It can be seen from these data that, in the studied range of vacuum arc discharge parameters, the deposition temperature increases almost linearly with an increase in the discharge current and absolute values of the negative potential and a decrease in the distance between the cathode and the substrate.

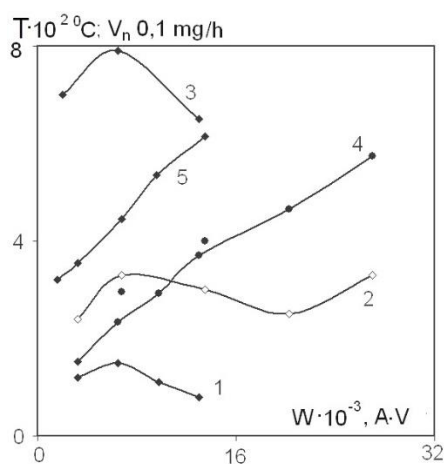


Fig. 1. Dependence of the rate (1–3) and temperature (4, 5) of coatings deposition on the arc current and the bias potential on the substrates at different distances from the cathode: 1 – $I=65 \text{ A}$, $L=300 \text{ mm}$; 2 – $I=135 \text{ A}$, $L=300 \text{ mm}$; 3 – $I=65 \text{ A}$, $L=200 \text{ mm}$; 4 – $I=65 \text{ A}$, $L=300 \text{ mm}$; 5 – $I=135 \text{ A}$, $L=200 \text{ mm}$

The rate of coating deposition increases with an increase in the arc current and a decrease in the cathode–substrate distance and decreases with an increase in the absolute values of the potential. The relationship between these parameters can be determined by the analytical relationship:

$$V = \alpha V_0 \xi, \quad (1)$$

where $\alpha = (1.641 - 0.58\gamma + 0.468\gamma^2) - (0.197 - 0.057\gamma - 0.038\gamma^2) \cdot \beta$; $V_0 = (56 + 113.2\gamma - 124.4\gamma^2) - (14.5 + 40.4\gamma - 44.8\gamma^2) \cdot \beta$; $\xi = 0.0154 I_d$; $\gamma = 10^{-2} U$; $\beta = 10^{-2} R_0$.

The arc current (I_d) is measured in A, the biaspotential (U) in V, the distance from the cathode surface to the sample (R) in mm.

For options for placing plasma sources in the formation of coatings on long parts, results can be obtained based on the approaches proposed in [15], as shown in Fig. 2.

So, with an arbitrary arrangement of two samples, as shown in Fig. 2, the calculated mass flow comes from the surface of the cathode element dF_1 to the surface of the sample dF_2 using the equation:

$$dm_{1,2} = A \frac{\cos \varphi_1 \cdot \cos \varphi_2}{\pi r^4} dF_1 \cdot dF_2, \quad (2)$$

where A is the amount of substances entering the hemispherical space. After integrating (2) over the cathode and sample surfaces, we obtain:

$$M_0 = A \frac{\cos^4 \varphi_1}{R_0^2} F_1 F_2. \quad (3)$$

It can be seen that the rate of coating deposition will be inversely proportional to the square of the distance between the sample and the cathode surface R_0^2 and proportional to $\cos^4 \varphi_1$.

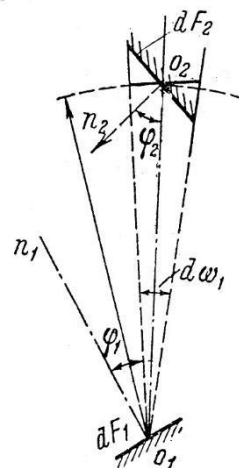


Fig. 2. Arrangement of two samples dF_1 , dF_2

Fig. 3 shows the results of comparisons of the experimental data with the data obtained by relation (3) for the samples installed along the axis of the system and with a surface parallel to the cathode surface. Relative rate of coating formation $\psi = v_1/v_0$ and the relative distance between the cathode and substrate surfaces $\eta = R_1/R_0$ (R_0 is the distance to the initial sample).

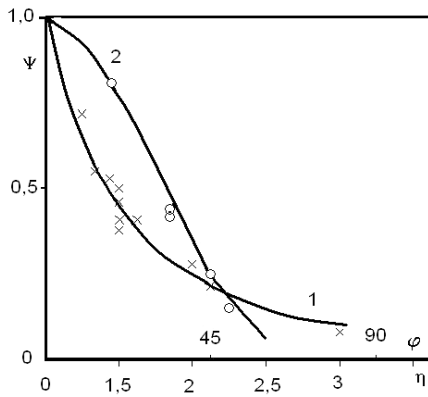


Fig. 3. Dependence of the relative rate of coating deposition – ψ on the relative distance between the cathode and substrate – η (1) and on the angle of the sample ϕ (2)

It can be seen from Fig. 3 that for coatings formed during the operation of one plasma source, the dependence ψ on η and ϕ corresponds to relation (3), but there is some dependence on the value of the negative potential on the sample for ψ at $\eta = 1.5$.

For coatings deposited on substrates located at 45° angle to the cathode surface and at different distances (l) from the normal to its surface, the following relations are established:

for $\frac{l}{R_0} = 0.086$, $\frac{V}{V_0} = 0.84$, and accordingly $0.17 \dots 0.8$; $0.25 \dots 0.76$; $0.34 \dots 0.76$; $0.43 \dots 0.7$.

The data obtained show that in the range of values of l corresponding to angles of about 20° , the deposition rate is 1.2 times lower compared to the rates of deposition on substrates parallel to the cathode surface. The established features are due to a change in the ratio between the ionic component of the vacuum arc discharge, the amount of macroparticles and neutral gas in the coating formation zone.

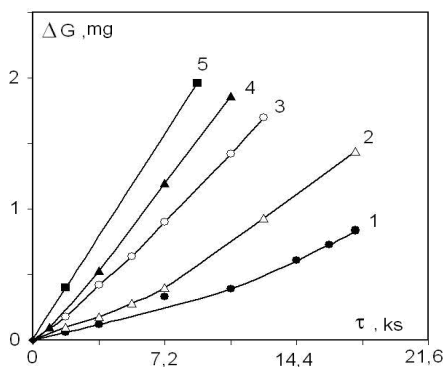


Fig. 4. Kinetic curves of coatings erosion formed at a discharge current of 70 (1 – 4) and 135 A (5). Substrate temperature: 1 – 256; 2 – 326; 3 – 466; 4 – 543; 5 – 673 °C

For coatings formed on substrates, the surfaces of which are parallel to the cathode surface, measurements of technological characteristics, in particular, microhardness and erosion rate during cavitation, were carried out. Typical kinetic curves of coatings erosion are shown in Fig. 4. The kinetic curves for coatings changes

with a change in the deposition temperature. Cavitation erosion increased with increasing deposition temperature and arc current.

The dependence of microhardness and cavitation erosion rate of the coatings from depositing temperature is shown on Fig. 5.

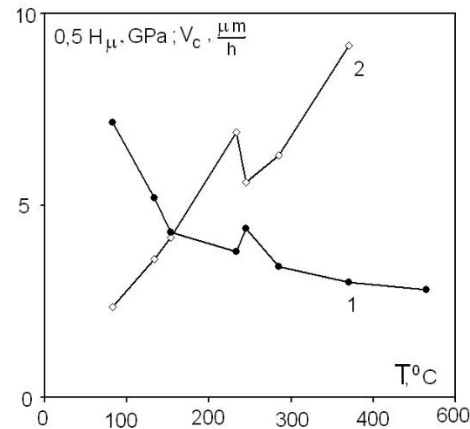


Fig. 5. Dependence of microhardness (1) and cavitation wear rate (2) on the temperature of coatings deposition

The data in Fig. 5 show that with increasing deposition temperature, there is a decrease in the microhardness of the Ti-coatings (H_μ) and an increase in cavitation wear rate (V_C). At a temperature of about 250°C , a feature is observed in the course of the curves, which, as studies have shown, is due to a change in the structure of the coatings and the possibility of the dynamic strain aging factor.

Table 1 presents the values of relative microhardness H_μ , resistance to wear under the action of abrasive Z_A and cavitation Z_C for coating samples obtained on substrates located at 45° angle of relative to the cathode surface and at different distances from the normal to the cathode surface. Table 1 shows that the nature of the dependences of H_μ , Z_C , Z_A on ϕ coincides and, as studies have shown, are due to the structural features of the coatings (Fig. 6).

Table 1
Relative mechanical characteristics of titanium coatings depending on the angle of location with respect to the plasma source

ϕ	0	$4^\circ50'$	$9^\circ40'$	14°	$18^\circ50'$	$23^\circ30'$
H_μ	1	0.98	1	1.05	1.07	1.17
Z_C	1	1.45	1.28	1.32	1.56	1.58
Z_A	1	0.78	0.76	0.86	0.94	1.07

Surface microphotographs of the samples in Fig. 6 show the presence of a significant amount of macroparticles and changes in their number at different potentials on the substrate, where the coating is formed, and the arc current. An increase in the bias potential on the substrate leads to a decrease in the number and size of macroparticles, and an increase in current, on the contrary, leads to an increase in their size and number.

Fig. 7 shows the change in the surface topography of coatings during cavitation erosion and it can be seen that, first of all, destruction begins at macro defects, which can be the boundaries of macroparticles.

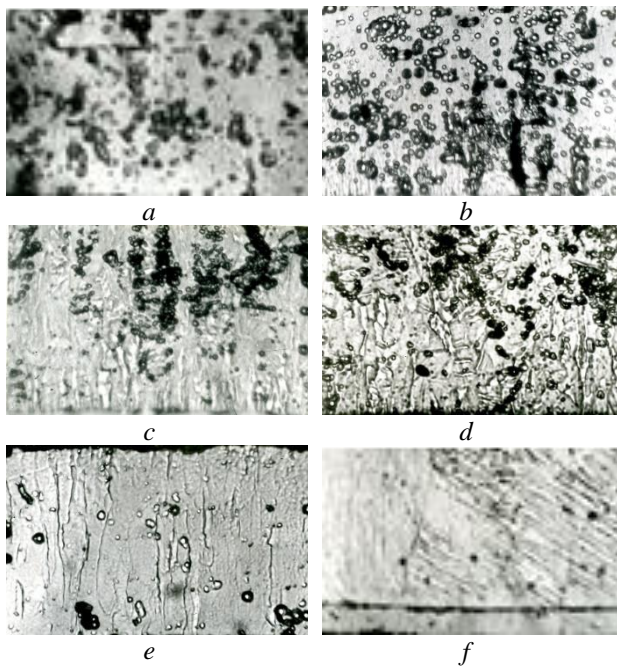


Fig. 6. Micrographs of the structure of Ti coatings ($\times 1000$): $I=65$ A (a, c, e), $I=135$ A (b, d, f); $U=50$ (a, b), 100 (c, d), and 200 V (e, f)

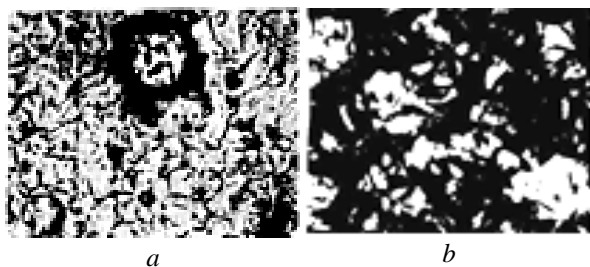


Fig. 7. Surface topography of Ti coatings ($\times 1000$): a – initial sample; b – after cavitation erosion for 1.8 ks

The results of studies of the magnitude of cavitation erosion of the Ti-Al coatings are presented in Fig. 8.

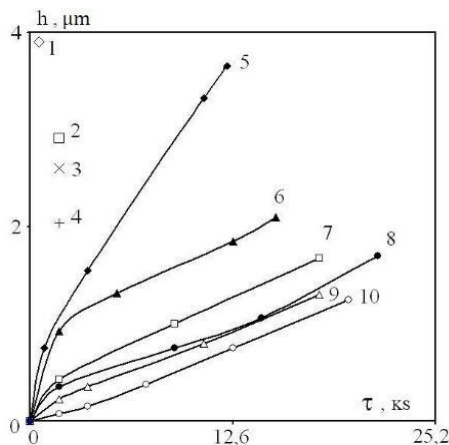


Fig. 8. Kinetic curves of cavitation destruction of coatings Al (1–4), Ti-Al (5–7, 9, 10), Ti-Al (8) cathode. $I(\text{Al})=70$ A (3, 5–7, 9, 10); $I(\text{Ti})=100$ (5, 6, 10), 85 (7), 120 A (9); $P_{Ar}=8 \cdot 10^{-3}$ (1–5), $4.6 \cdot 10^{-2}$ (6–9), 0.8 (10) Pa. The values of h are reduced by a factor of 5 for 1–4 samples, and for sample 5, by a factor of 2

Data in Fig. 8 show that only Al (2–4) coatings have high cavitation erosion rates. The rate of erosion of the coatings deposited on the substrate installed on the axis of the chamber (2) is 1.4 times higher than the rate of coating erosion (4) deposited on the axis at a distance of 140 mm, which is obviously determined by the change in the number of interstitial atoms in the coatings. Titanium coatings with additionally introduced Al have lower destruction rates. With the same parameters of the vacuum-arc discharge, the pressure in the vacuum chamber has a significant effect. Coatings deposited at higher pressures have poor erosion resistance (5, 6). With an increase in the current of the titanium cathode at a constant current of the aluminum cathode, the rate of erosion of the formed coatings with a thickness of 9...15 μm decreases (7, 9, 10).

Coatings up to 15 μm thick, obtained on the basis of Ti with Al additions, have an average erosion rate under cavitation equal to 0.25 $\mu\text{m}/\text{h}$, which is 2.6 times less than the minimum value for titanium samples, i.e. they can be used for their protection.

The study of abrasive wear of coatings of the Ti-Al system and only from Ti, which are deposited on substrates at close parameters of the vacuum-arc discharge, showed that the wear rate of Ti-Al coatings is 2.5–3 times less than that of titanium coatings.

Ti and Zr coatings deposited at a current of 100 A, pressure in a vacuum chamber of $7 \cdot 10^{-4}$ Pa, and in a direct flow of ions, have a thickness that decreases with increasing distance from the system axis much faster compared to the TiZr coating, which is formed at an angle of incidence on the substrate of ion fluxes equal to 45° . The dependence of the erosion depth of TiZr coatings from the time of cavitation wear is shown in Fig. 9.

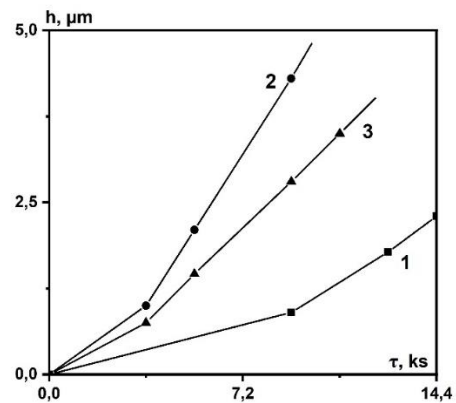


Fig. 9. Kinetic curves of destruction of coatings under the cavitation: 1 – Ti; 2 – Zr; 3 – TiZr

From Fig. 9 it can be seen that for the same time, the effect of cavitation erosion of coatings occurs at different rates. The zirconium coating has the highest erosion rate, the titanium has the lowest one, and the combined TiZr is destroyed at a rate less than the Zr coating, but more than the Ti coating.

Coatings based on Ti-Ni system were deposited, in the composition of which the amount of Ni was changed in the range of 30...50 at.%. Fig. 10 shows X-ray diffraction pattern of the Ti-Ni coating with a nickel concentration of about 50 at.%.

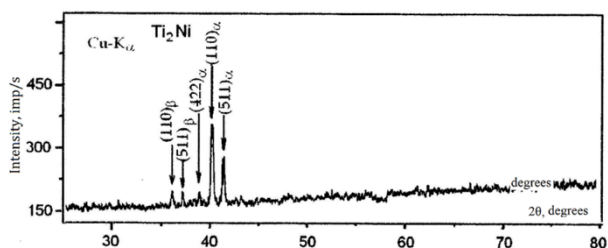


Fig. 10. X-ray diffraction pattern of the Ti-Ni coating

It can be seen (see Fig. 10) that there are diffraction peaks from the (422) and (511) planes and from the (110) plane of the molybdenum substrate. Planes (422) and (511) belong to the Ti_2Ni compound, which has complex fcc a $(FeW)_3C$ -type structure lattice and contains 96 atoms per unit cell. An increase in the background with an increase in the angle 2θ indicates a multiphase composition of the condensate, in which, along with the δ phase, there can be γ -TiNi phases, an α -solid solution of Ti in Ni (up to 9.4 at.% Ti), as well as pure α -Ti. The presence of the last phase indicates the absence of a ferromagnetic state of the coatings, and the presence of multiphase causes an increase in crystallization centers, which ensures a high dispersion of the coating at the level of the amorphous state. The obtained structural data are in good agreement with the results of structural studies of vacuum-arc coatings deposited from the one alloy cathode $Ti_{50}Ni_{50}$ [16].

Studies of the erosion of TiNi coatings under cavitation conditions have shown that during the formation of coatings with a micro hardness somewhat less than 8 GPa, the cavitation erosion resistance of the coatings is $Z_h = 2.0$. With an increase in microhardness up to 10 GPa, the erosion resistance rapidly decreases. So, at $H_\mu = 5.3$ GPa $Z_C = 2.85$, at $H_\mu = 7.5$ GPa $Z_C = 2.38$, and at $H_\mu \sim 10$ GPa $Z_C \sim 0.12$.

On the basis of experimental data on microhardness, cavitation and abrasive wear, the erosion resistance of coatings relative to pure titanium during cavitation action (Z_C) and rigidly fixed abrasive particles (Z_A) was calculated (Table 2).

Table 2

Mechanical characteristics of coatings:
Ti, TiAl, TiZr, and TiNi

Characteristics	Ti	TiAl	TiZr	TiNi
H_μ , GPa	1.64	4.5	1.8	5.3
Z_C	1.25	4.62	0.7	2.85
Z_A	1.07	3.21	1.1	3.01

The alloyed coatings of the TiAl and TiNi systems with a microhardness of 4.5 and 5.3 GPa, respectively, have the highest resistance to cavitation and abrasive wear among the studied coatings (see Table 2).

CONCLUSIONS

The effect of technological parameters of the deposition process (cathode-substrate distance, substrate temperature, shear stress, arc current) on the deposition rate, microhardness, and cavitation erosion resistance of vacuum-arc titanium coatings has been studied. The deposition rate of titanium coatings from one cathode is

inversely proportional to the square distance between the sample and the cathode surface R_0^2 and is proportional to $\cos^4 \varphi_I$, where φ is the angle of inclination of the sample relative to the normal to the cathode surface.

It is shown that titanium coatings deposited at a temperature of ~ 250 °C, at a distance of 200 mm from the cathode, at arc current of ~ 100 A and a bias potential of -200 V have the highest cavitation erosion resistance.

Among the investigated vacuum-arc coatings Ti, TiAl, TiZr, and TiNi, the coating of the TiAl and TiNi systems with a microhardness of 4.5 and 5.3 GPa, respectively, have the highest resistance to cavitation and abrasive wear.

REFERENCES

1. P. Kumar, P.R. Saini. Study of cavitation in hydro turbines: A review // *Renewable and Sustainable Energy Reviews*. 2010, v. 14, p. 374-383.
2. L. Yea, X. Zhua, Y. Hea, X. Wei. Ultrasonic cavitation damage characteristics of materials and a prediction model of cavitation impact load based on size effect // *Ultrasonics-Sonochemistry*. 2020, v. 66, p. 105115.
3. I.O. Klimenko, V.G. Marinin, V.D. Ovcharenko, V.I. Kovalenko, A.S. Kuprin, O.M. Reshetnyak, V.A. Belous, H.Yu. Rostova. Resistance of titanium alloys to cavitation wear // *Problems of Atomic Science and Technology*. 2022, N 1(137), p. 130-135.
4. Sh. Hattori, T. Kitagawa. Analysis of cavitation erosion resistance of cast iron and nonferrous metals based on database and comparison with carbon steel data // *Wear*. 2010, v. 269, p. 443-448.
5. W.H. Xian, D.G. Li, D.R. Chen. Investigation on ultrasonic cavitation erosion of TiMo and TiNb alloys in sulfuric acid solution // *Ultrasonics Sonochemistry*. 2020, v. 62, p. 104877.
6. V.I. Kovalenko, V.G. Marinin. Investigation of the fracture for the doped titanium alloys under the influence of cavitation // *Eastern European Journal of Advanced Technologies*. 2015, v. 78, N 6/11, p. 4-8.
7. A.S. Kuprin, V.D. Ovcharenko, S.A. Leonov, G.N. Tolmachova, V.A. Belous, E.N. Reshetnyak, I.O. Klimenko, M. Kmech. Cavitation erosion of Ti-6Al-4V alloy with vacuum-arc TiN and CrN coatings // *Problems of Atomic Science and Technology*. 2018, v. 117, N 5, p. 103-108.
8. A. Krella. Resistance of PVD Coatings to Erosive and Wear Processes: A Review // *Coatings*. 2020, v. 10, p. 921.
9. A.K. Krella. Cavitation erosion of monolayer PVD coatings – An influence of deposition technique on the degradation process // *Wear*. 2021, v. 478-479, p. 203762.
10. V.G. Marinin, V.I. Kovalenko, N.S. Lomino, Yu.A. Zadneprovsky, V.D. Ovcharenko. Cavitation erosion of Ti coatings produced by the vacuum arc method // *International Symposium on Discharges and Electrical Insulation in Vacuum, ISDEIV*. 2000, v. 2, p. 567-570.
11. V.A. Belous, V.N. Voyevodin, V.M. Khoroshikh, G.I. Nosov, V.G. Marinin, S.A. Leonov, V.D. Ovcharenko, V.I. Kovalenko, A.A. Komar, A.S. Kuprin,

L.O. Shpagina. Prototype equipment and techniques for obtaining cavitation-resistant coatings to be applied to working surfaces of steam turbine blades made of VT6 titanium alloy in order to replace imported counterparts // *Sci. Innov.* 2016, v. 12(4), p. 27-35.

12. R.H. Richman, A.S. Rao, D.E. Hodgson. Cavitation erosion of two NiTi alloys // *Wear.* 1992, v. 157 (2), p. 401-407.

13. J. Stella, E. Schuller, C. Hebing, O.A. Hamed, M. Pohl, D. Stover. Cavitation erosion of plasma-sprayed NiTi coatings // *Wear.* 2006, v. 260, p. 1020-1027.

14. L.M. Yang, A.K. Tieu, D.P. Dunne, S.W. Huang, H.J. Li, D. Wexler, Z.Y. Jiang. Cavitation erosion resistance of NiTi thin films produced by Filtered Arc Deposition // *Wear.* 2009, v. 267, p. 233-243.

15. A.G. Bloch. *Fundamentals of heat transfer by radiation.* М.: "Gosenergoizdat", 1962, 332 p.

16. J.L. He, K.W. Won, J.T. Chang. TiNi thin films prepared by cathodic arc plasma ion plating // *Thin Solid Films.* 2000, v. 359, p. 46-54.

Article received 29.06.2022

КАВИТАЦІЙНА ТА ЕРОЗІЙНА СТІЙКІСТЬ ВАКУУМНО-ДУГОВИХ ПОКРИТТІВ Ti, Ti-Al, Ti-Zr І Ti-Ni

І.О. Клименко, В.Г. Маринін, М.О. Бортницька, О.С. Куррін

Дослідження впливу технологічних параметрів осадження (відстань катод-підкладка, температури підкладки, напруги зсуву, струму дуги) вакуумно-дугових титанових покриттів показали, що швидкість осадження з одного катода обернено пропорційна квадратів відстані між зразком та поверхнею катода і пропорційна куту нахилу зразка відносно нормалі до поверхні катода. Титанові покриття, які осадженні при оптимальних параметрах, у 1,25 рази мають вищу кавітаційну стійкість, ніж масивний титан. Серед легованих вакуумно-дугових покриттів TiAl, TiZr і TiNi найбільшу стійкість до кавітаційного та абразивного зносу мають покриття систем TiAl та TiNi.